Carcinogenesis vol.31 no.3 pp.342–349, 2010
doi:10.1093/carcin/bgp179
Advance Access publication July 28, 2009

IGFBP7 is a p53-responsive gene specifically silenced in colorectal cancer with CpG island methylator phenotype

Hiromu Suzuki[1,2,3], Shinichi Igarashi[1], Masanori Nojima[4], Reo Maruyama[1], Eiichiro Yamamoto[1], Masahiro Kai[2], Hirofumi Akashi[5], Yoshiyuki Watanabe[6], Hiroyuki Yamamoto[1], Yasushi Sasaki[3], Fumio Itoh[6], Kohzoh Imai[1], Tamotsu Sugai[7], Lanlan Shen[8], Jean-Pierre J.Issa[8], Yasuhisa Shinomura[1], Takashi Tokino[3] and Minoru Toyota[2,*]

[1]First Department of Internal Medicine, [2]Department of Biochemistry, [3]Department of Molecular Biology, Cancer Research Institute, [4]Department of Public Health and [5]Center for Bioinformation, Sapporo Medical University, South 1,West 17, Chuo-ku, Sapporo 060-8556, Japan, [6]Department of Gastroenterology and Hepatology, St Marianna University School of Medicine, Kawasaki 216-8511, Japan, [7]Division of Diagnostic Molecular Pathology, Department of Pathology, Iwate Medical University, Morioka 020-8505, Japan and [8]Department of Leukemia and Epigenetics Center, University of Texas M. D. Anderson Cancer Center, Houston, TX 77030, USA

*To whom correspondence should be addressed. Tel: +81 11 611 2111 ext. 2680; Fax: +81 11 622 1918;
Email: mtoyota@sapmed.ac.jp
Correspondence may also be addressed to Yasuhisa Shinomura.
Tel: +81 11 611 2111 ext. 3210; Fax: +81 11 611 2282;
Email: shinomura@sapmed.ac.jp

A subset of colorectal cancers (CRCs) show simultaneous methylation of multiple genes; these tumors have the CpG island methylator phenotype (CIMP). CRCs with CIMP show a specific pattern of genetic alterations, including a high frequency of *BRAF* mutations and a low frequency of *p53* mutations. We therefore hypothesized that genes inactivated by DNA methylation are involved in the BRAF- and p53-signaling pathways. Among those, we examined the epigenetic inactivation of insulin-like growth factor-binding protein 7 (*IGFBP7*) expression in CRCs. We found that in CRC cell lines, the silencing of *IGFBP7* expression was correlated with high levels of DNA methylation and low levels of histone H3K4 methylation. Luciferase and chromatin immunoprecipitation assays in unmethylated cells revealed that p53 induces expression of *IGFBP7* upon binding to a p53 response element within intron 1 of the gene. Treating methylated CRC cell lines with 5-aza-2′-deoxycytidine restored p53-induced *IGFBP7* expression. Levels of *IGFBP7* methylation were also significantly higher in primary CRC specimens than in normal colonic tissue ($P < 0.001$). Methylation of *IGFBP7* was correlated with BRAF mutations, an absence of p53 mutations and the presence of CIMP. Thus, epigenetic inactivation of *IGFBP7* appears to play a key role in tumorigenesis of CRCs with CIMP by enabling escape from p53-induced senescence.

Introduction

Colorectal cancer (CRC) arises through the accumulation of multiple genetic changes, including mutation of *APC*, *K-ras* and *p53* (1). In addition to genetic changes, however, epigenetic alterations such as DNA methylation also play a role through the silencing of cancer-related genes (2–4). Moreover, a subset of CRCs show methylation of multiple genes, which has been termed the CpG island methylator phenotype (CIMP, ref. 5). Tumors with CIMP show distinct pattern of genetic alterations, including a high frequency of *K-ras* and *BRAF* mutations and a low frequency of *p53* mutations (6–8). The molecular mechanism underlying this pattern of mutations remains unknown.

Senescence is a state of permanent growth arrest in which cells are refractory to mitogenic stimuli. Although activation of Ras exerts a mitogenic effect in immortalized cells, expression of oncogenic Ras provokes stress responses in primary cells that results in irreversible growth arrest termed premature senescence (9,10). In most cell types, activation of p53 is crucial for initiating senescence in response to DNA damage, and it has been shown that p53-mediated senescence is caused by induction of target genes such as *p21WAF1/CDKN1A*, *PAI-1* and *DEC-1* (11,12).

p53 is a transcription factor that induces expression of various genes involved in cell cycle checkpoints, apoptosis and DNA repair (13), and a variety of approaches, including differential display, representational difference analysis and complementary DNA (cDNA) microarray, have been used to identify its targets. p53 acts by binding to so-called p53 response elements (p53REs), which consist of two copies of a 10 bp motif, separated by 0–12 bp. Using the p53RE as a probe, we previously employed an in silico approach to identify the vitamin D receptor gene as a transcriptional target of p53 (14), which confirmed the utility of the in silico analysis for identification of p53 target genes within the human genome.

Insulin-like growth factor-binding protein 7 (IGFBP7; also called IGFBP-r1 or MAC25) can inhibit proliferation of cancer cells, and its expression is downregulated in various types of tumors (15,16). For instance, *IGFBP7* is silenced by DNA methylation in both colorectal and gastric cancers (17,18). Although the function of IGFBP7 in tumorigenesis is not fully understood, Wajapeyee *et al.* (19) recently reported that expression of activated BRAF in primary melanocytes leads to synthesis of IGFBP7, which then acts through autocrine/paracrine pathways to inhibit extracellular signal-regulated kinase signaling and induce senescence and apoptosis in BRAF-activated cells. Our findings in the present study indicate that *IGFBP7* is a direct target of p53, suggesting that IGFBP7 is a mediator of p53-dependent growth suppression and that epigenetic inactivation of *IGFBP7* is a potentially useful molecular target for the diagnosis and treatment of CRCs with CIMP.

Materials and methods

Cell lines and tissue specimens

A set of nine CRC cell lines (CaCO2, Colo320, DLD1, HCT116, HT29, LoVo, RKO, SW48 and SW480) and a lung cancer cell line (H1299) were obtained and cultured as described previously (14,20). HCT116 cells harboring genetic disruptions within the *DNA methyltransferase 1 (DNMT1)* and *DNMT3B* loci (DKO2) (21) and within the *TP53* locus (22) have been described previously. A total of 87 primary CRCs, 49 colorectal adenoma and 41 normal colon specimens were collected as described previously (7). Informed consent was obtained from all patients before collection of the specimens. Genomic DNA was extracted using the standard phenol–chloroform procedure. Total RNA was extracted using TRIZOL reagent (Invitrogen, Carlsbad, CA) and then treated with a DNA-free kit (Ambion, Austin, TX). Genomic DNA and total RNA from normal colon tissue from a healthy individual were purchased from BioChain (Hayward, CA).

Drug treatment

To analyze restoration of *IGFBP7* gene expression, CRC cells were treated with 2 μM 5-aza-2′-deoxycytidine (DAC) (Sigma, St Louis, MO) for 72 h, replacing the drug and medium every 24 h. To determine whether *IGFBP7* is upregulated by endogenous p53, wild-type and $p53^{-/-}$ HCT116 cells were treated with 0.1 μM DAC for 48 h, replacing the drug and medium 24 h after the beginning of treatment. This was followed by addition of adriamycin (ADR) to a final concentration of 0.5 μg/ml and incubation for an additional 24 h.

In silico identification of p53RE

A p53RE database was created as described previously (14). Briefly, human genome sequence data were downloaded from the National Center for

Abbreviations: ADR, adriamycin; cDNA, complementary DNA; ChIP, chromatin immunoprecipitation; CIMP, CpG island methylator phenotype; CRC, colorectal cancer; DAC, 5-aza-2′-deoxycytidine; DNMT1, DNA methyltransferase 1; IGFBP7, insulin-like growth factor-binding protein 7; mRNA, messenger RNA; MSP, methylation-specific polymerase chain reaction; PCR, polymerase chain reaction; p53RE, p53 response element.

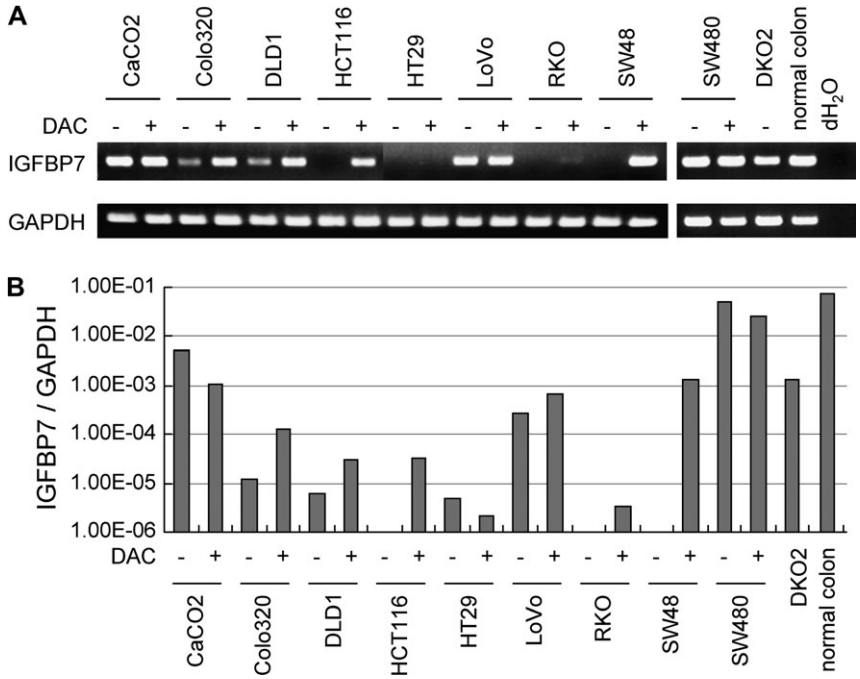

Fig. 1. Analysis of *IGFBP7* expression in CRC cell lines. (**A**) Reverse transcriptase–PCR analysis of *IGFBP7* in the indicated CRC cell lines. Expression of *IGFBP7* was examined using cDNA prepared from CRC cell lines treated with mock (−) or 1.0 μM DAC (+). Glyceraldehyde-3-phosphate dehydrogenase (GAPDH) expression was used as a control to confirm the integrity of the RNA. (**B**) Real-time PCR analysis of *IGFBP7*. The results were normalized using levels of glyceraldehyde-3-phosphate dehydrogenase expression as control.

Biotechnology Information Human Assembly 33. Stored in the p53RE database were sequences containing fewer than four mismatches in the 20 nucleotide p53RE consensus sequence and a spacer of fewer than 12 bp between the two 10 bp motifs. We then analyzed the distribution of p53REs with respect to transcription start sites for *IGFBP7*, taking into consideration the number of mismatches and the length of the spacers.

Reverse transcriptase–polymerase chain reaction

Single-stranded cDNA was prepared using SuperScript III reverse transcriptase (Invitrogen), and the integrity of the cDNA was confirmed by amplifying glyceraldehyde-3-phosphate dehydrogenase (*GAPDH*). Polymerase chain reaction (PCR) was run in a 50 μl volume containing 100 ng of cDNA, 1× Ex Taq Buffer (TaKaRa, Otsu, Japan), 0.3 mM deoxynucleoside triphosphate, 0.25 μM each primer and 1 U of TaKaRa Ex Taq Hot Start Version (TaKaRa). The PCR protocol entailed 5 min at 95°C; 35 cycles of 1 min at 95°C, 1 min at 55°C and 1 min at 72°C; and a 7 min final extension at 72°C. Primer sequences and PCR product sizes are shown in supplementary Table 1 (available at *Carcinogenesis* Online).

Real-time reverse transcriptase–PCR

Real-time reverse transcriptase–PCR was carried out using TaqMan Gene Expression Assays (Applied Biosystems, Carlsbad, CA) and 7900HT Fast Real-Time PCR System (Applied Biosystems) according to the manufacturer's instructions. SDS2.2.2 software (Applied Biosystems) was used for comparative ΔCt analysis, and *GAPDH* served as an endogenous control.

Methylation analysis

Genomic DNA (2 μg) was modified with sodium bisulfite using an EpiTect Bisulfite Kit (Qiagen, Hilden, Germany). Methylation-specific polymerase chain reaction (MSP) and bisulfite sequencing analysis were performed as described previously (23). Bisulfite sequencing and PCR products were cloned into pCR2.1-TOPO vector (Invitrogen), and 8–12 clones from each sample were sequenced using an ABI3130x automated sequencer (Applied Biosystems).

Bisulfite pyrosequencing was carried out as described previously (20) using primers designed with PSQ Assay Design software (Biotage, Uppsala, Sweden). After PCR, the biotinylated products were purified, made single stranded and used as a template in the pyrosequencing reaction run according to the manufacturer's instructions. The PCR products were bound to Streptavidin Sepharose beads HP (Amersham Biosciences, Piscataway, NJ), after which beads containing the immobilized PCR product were purified, washed and denatured using a 0.2 M NaOH solution. After addition of 0.3 μM sequencing primer to the purified PCR product, pyrosequencing was carried out using a PSQ96MA system (Biotage) and Pyro Q-CpG software (Biotage). Primer sequences and PCR product sizes are shown in supplementary Table 1 (available at *Carcinogenesis* Online).

Chromatin immunoprecipitation

Chromatin immunoprecipitation (ChIP) was carried out using a ChIP Assay Kit (Upstate Biotechnology, Lake Placid, NY) with anti-trimethylated histone H3K4 monoclonal antibody (clone MC315; Upstate, Lake Placid, NY) or anti-human p53 monoclonal antibody (DO-1; Santa Cruz Biotechnology, Santa Cruz, CA) as described previously (14,20,24). For histone methylation analysis, HCT116 cells treated with or without DAC and DKO2 cells were used as described previously (20). For p53 analysis, DLD1 cells infected with recombinant adenovirus Ad-p53 or Ad-LacZ were used (14). Briefly, the protein and DNA in 2×10^6 cells were cross-linked in a 1% formaldehyde solution for 15 min at 37°C. The cells were then lysed in 200 μl of sodium dodecyl sulfate lysis buffer and sonicated to generate 300–800 bp DNA fragments. After centrifugation, the cleared supernatant was diluted 10-fold with ChIP dilution buffer, after which one-fiftieth of the extract volume was used for PCR amplification as the input control. The remaining extract was incubated with specific antibody for 16 h at 4°C. Immune complexes were precipitated, washed and eluted as recommended. DNA–protein cross-links were reversed by heating for 4 h at 65°C, after which the DNA fragments were purified and dissolved in 50 μl of Tris–ethylenediaminetetraacetic acid. One microliter of each sample was used as a template for PCR amplification. Real-time PCR for histone analysis was carried as described previously (20) using the primers listed in supplementary Table 1 (available at *Carcinogenesis* Online). PCR amplification of *IGFBP7* containing the putative p53RE was also carried out using primers listed in supplementary Table 1 (available at *Carcinogenesis* Online).

Luciferase assays

Reporter plasmids pGL3-RE-*IGFBP7* and pGL3-RE-*IGFBP7*-mut were constructed as follows. Three tandem repeats of RE-*IGFBP7* (5′-AAACAAGTCCAAGCTTGCTG-3′) and its unresponsive mutant form, RE-*IGFBP7*-mut (5′-AAAAAATTCCAAGATTTCTG-3′), were synthesized and inserted upstream of a basal SV40 promoter in the pGL3-promoter vector (Promega, Madison, WI), yielding pGL3-RE-*IGFBP7* and pGL3-RE-*IGFBP7*-mut, respectively. Using Lipofectamine 2000 (Invitrogen), H1299 cells (5×10^4 cells per well in 24-well plates) were transfected with 100 ng of one of the reporter plasmids, 100 ng of pcDNA-p53 or an empty vector and 2 ng of pRL-TK (Promega). Luciferase activities were measured 48 h after transfection using a Dual-Luciferase Reporter Assay System (Promega). The ability to stimulate transcription was determined

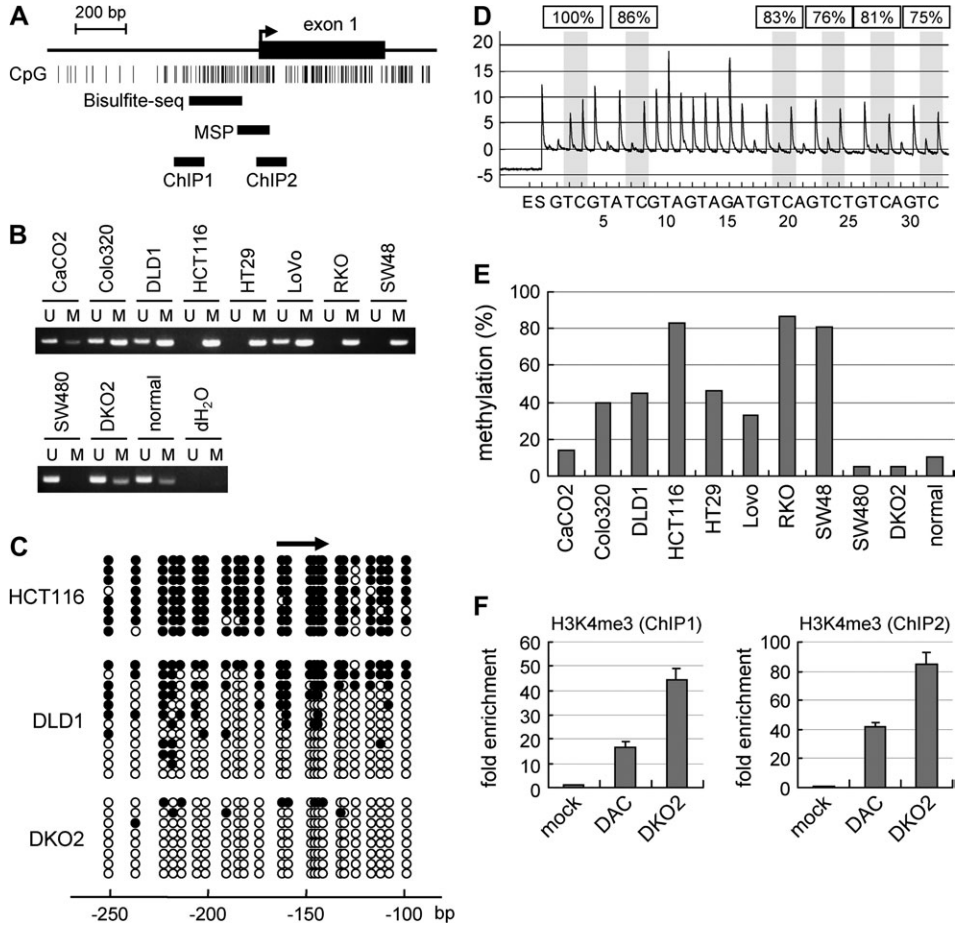

Fig. 2. Methylation analysis of *IGFBP7*. (**A**) Schematic representation of the 5′ region of *IGFBP7*. CpG sites are shown as vertical bars. The regions analyzed by bisulfite sequencing, MSP and ChIP are indicated by solid bars. The transcription start site is indicated by an arrow. (**B**) MSP analysis of *IGFBP7* in CRC cell lines. The cell lines examined are shown on the top. (**C**) Bisulfite sequencing of IGFBP7. Open and filled circles represent unmethylated and methylated CpG sites, respectively. (**D**) Representative pyrogram for *IGFBP7*. Gray columns indicate regions with C to T polymorphic sites. The percentage of methylation at each CpG site is shown at the top; *y*-axis, signal peaks proportional to the number of nucleotides incorporated and *x*-axis, the nucleotides incorporated. (**E**) Summary of pyrosequencing. *y*-axis, the percentages of methylated cytosines in the samples, as determined from pyrosequencing. (**F**) ChIP analysis of trimethylation of histone H3K4 in the 5′ region of IGFBP7. ChIP assays were performed using HCT116 cells treated with mock or DAC. DKO2 cells (*DNMT1*$^{-/-}$*DNMT3B*$^{-/-}$ HCT116 cells) were also used.

from the ratio of luciferase activity in the cells transfected with the pGL3-RE-*IGFBP7* to the activity in the cells transfected with pGL3-RE-*IGFBP7*-mut. All experiments were performed in triplicate and repeated at least three times.

Expression vector

Full-length *IGFBP7* cDNA was PCR amplified using cDNA derived from DKO2 cells as a template. The PCR was run in a 50 µl volume containing 1× AccuPrime *Pfx* Reaction mix (Invitrogen), 0.3 µM each primer and 2.5 U of AccuPrime *Pfx* DNA polymerase (Invitrogen). The PCR protocol entailed 2 min at 95°C; 35 cycles of 15 s at 95°C, 30 s at 62°C and 1 min at 68°C; and a 5 min final extension at 68°C. Primer sequences are listed in supplementary Table 1 (available at *Carcinogenesis* Online). Amplified PCR products were then incubated with 1 U of Ex Taq DNA Polymerase (TaKaRa) for 10 min and cloned into pCR2.1-TOPO (Invitrogen). After the sequences were verified, fragments were cut using EcoRI and ligated into EcoRI-digested pcDNA3.1/HisA (Invitrogen).

Colony formation assays

Colony formation assays were carried out as described previously (25). Briefly, cells (1×10^5 cells) were transfected with 5 µg of one of the pcDNA3.1His-IGFBP7 vectors or with empty vector using Lipofectamine 2000 according to the manufacturer's instructions. Cells were then plated on 60 mm culture dishes and selected for 14 days with 0.6 mg/ml G418, after which the colonies that formed were stained with Giemsa and counted using National Institutes of Health IMAGE software.

Statistics

Statistical analyses were carried out using SPSSJ 15.0 (SPSS Japan, Tokyo, Japan). Pearson's correlation coefficient and *t*-test were used to evaluate the association between *IGFBP7* methylation. Methylation of *p16*, mutations of *p53*, mutations of *BRAF*, microsatellite instability and CIMP status were determined as described previously (5,7,26). Values of $P < 0.05$ were considered significant. To identify potentially distinct subgroups among colon cancer and adenoma patients, heat maps were constructed using K-means clustering method (27).

Results

Analysis of IGFBP7 expression in CRC cell lines

To test whether *IGFBP7* is epigenetically silenced in CRC, we first carried out an reverse transcriptase–PCR analysis with a set of CRC cell lines. We found that expression of *IGFBP7* messenger RNA (mRNA) was completely absent in four of the nine cell lines tested (HCT116, HT29, RKO and SW48) and was downregulated in two cell lines (Colo320 and DLD1) (Figure 1A). In many of the cells in which *IGFBP7* was downregulated, treatment with the DNA methyltransferase inhibitor DAC rapidly restored mRNA expression, which is indicative of epigenetic silencing of the genes through DNA methylation (Figure 1A). We also analyzed HCT116 cells in which the DNA methyltransferase genes *DNMT1* and *DNMT3B* were genetically disrupted (DKO2 cells), thereby abrogating DNA methylation (21). Those cells showed substantially greater expression of *IGFBP7* mRNA than the parental HCT116 cells (Figure 1A). In contrast to the cancer cells, *IGFBP7* was well expressed in normal colonic mucosa from a healthy individual (Figure 1A).

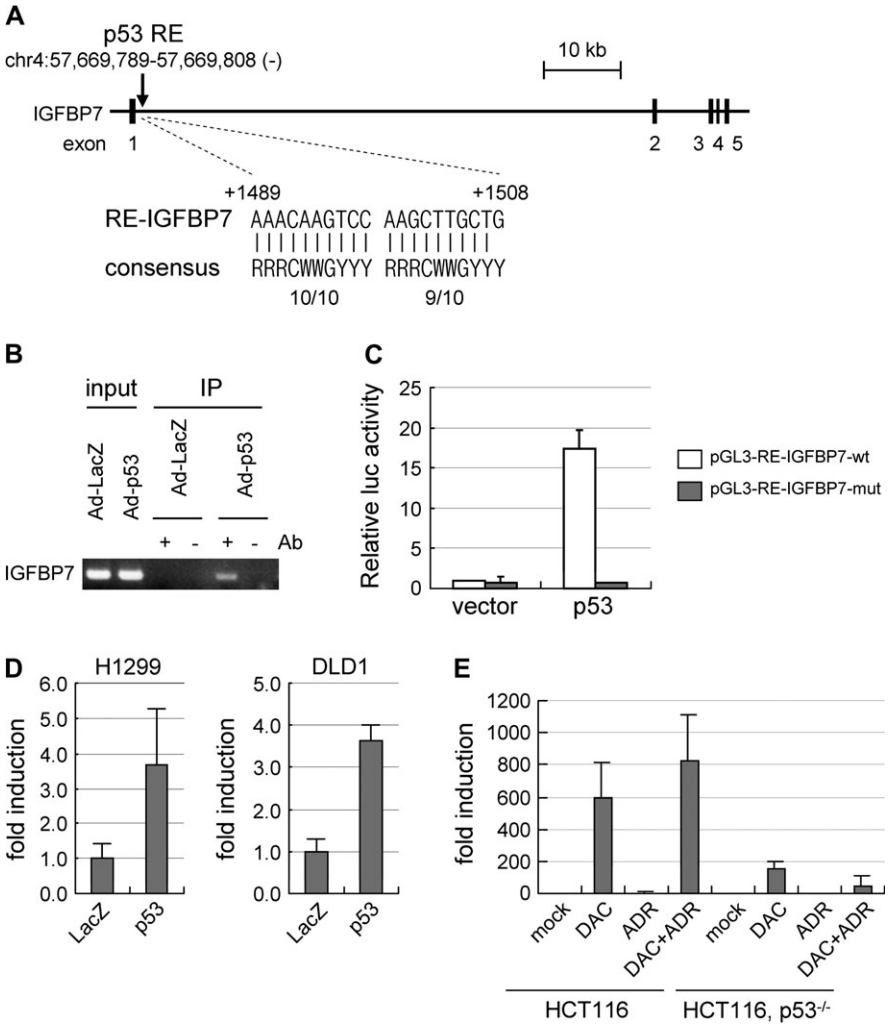

Fig. 3. Transcriptional activation of *IGFBP7* by p53. (**A**) In silico identification of p53REs. The structure of *IGFBP7* within the genome is shown. The putative p53RE in *IGFBP7* is shown as RE-*IGFBP7*. The nucleotide sequences of conserved p53REs are shown below (consensus). (**B**) ChIP analysis of *IGFBP7* p53RE. ChIP analysis was carried out using DLD-1 cells transfected with Ad-LacZ or Ad-p53, after which the chromatin was immunoprecipitated with anti-p53 antibody. The DNA was subjected to PCR using primers amplifying the region around RE-*IGFBP7*. (**C**) Luciferase assay for RE-*IGFBP7*. H1299 cells were cotransfected with empty vector or p53 plus pGL3-RE-*IGFBP7* or pGL3-RE-*IGFBP7*-mut. The relative luciferase activity was defined as the activity in the cells transfected with pGL3-RE-*IGFBP7* divided by the activity in cells transfected with pGL3-RE-*IGFBP7*-mut. (**D**) Induction of *IGFBP7* by p53. (**E**) Restoration of p53-induced *IGFBP7* expression by DAC.

When we then used TaqMan real-time reverse transcriptase–PCR to determine the relative levels of *IGFBP7* expression in the same samples, the results were consistent with those summarized above (Figure 1B), which strongly suggests that, in CRC, *IGFBP7* is a frequent target of epigenetic silencing through DNA methylation.

Analysis of IGFBP7 methylation in CRC cell lines

Because *IGFBP7* contains a CpG island in the region around its transcription start site, we next carried out MSP analysis using the primers illustrated in Figure 2A. We found that *IGFBP7* is completely or strongly methylated in the six CRC cell lines (Colo320, DLD1, HCT116, HT29, RKO and SW48) in which *IGFBP7* is silenced or downregulated (Figure 2B). In addition, detectable but relatively weak methylation was also found in cell lines (CaCO2, LoVo and DKO2) in which *IGFBP7* was expressed and in normal colonic mucosa (Figure 2B).

We verified the MSP results in selected samples using bisulfite sequencing, which revealed that the CpG island of *IGFBP7* is extensively methylated in CRC cell lines in which methylation was detected by MSP (Figure 2C). We also carried out a quantitative analysis of the methylation of six CpG sites located at the core of the CpG island using primers designed for bisulfite pyrosequencing (Figure 2D and E). The results confirmed the presence of high levels of methylation in cells in which *IGFBP7* expression was silenced or downregulated (DLD1, HCT116, HT29, RKO and SW48). In contrast, methylation levels were lower in cell lines in which *IGFBP7* was expressed (CaCO2, LoVo and SW480). DKO2 cells and normal colonic mucosa also showed low levels of *IGFBP7* methylation. In summary, we observed an inverse correlation between DNA methylation and *IGFBP7* expression in CRC cells.

To confirm that the CpG island is the promoter driving *IGFBP7* expression, we carried out ChIP–PCR to assess trimethylation of H3K4, which is reportedly a marker of active promoters (28). In both DAC-treated HCT116 cells and DKO2 cells, we observed significant enrichment of trimethylated H3K4 in the CpG island. In contrast, very little trimethylated H3K4 was detected in untreated HCT116 cells (Figure 2F).

Identification of IGFBP7 as a target gene of p53

We previously used a comparative genomic approach in which p53RE was employed as probe to identify novel p53 target genes (14). Using the same in silico analysis in the present study, we found a putative

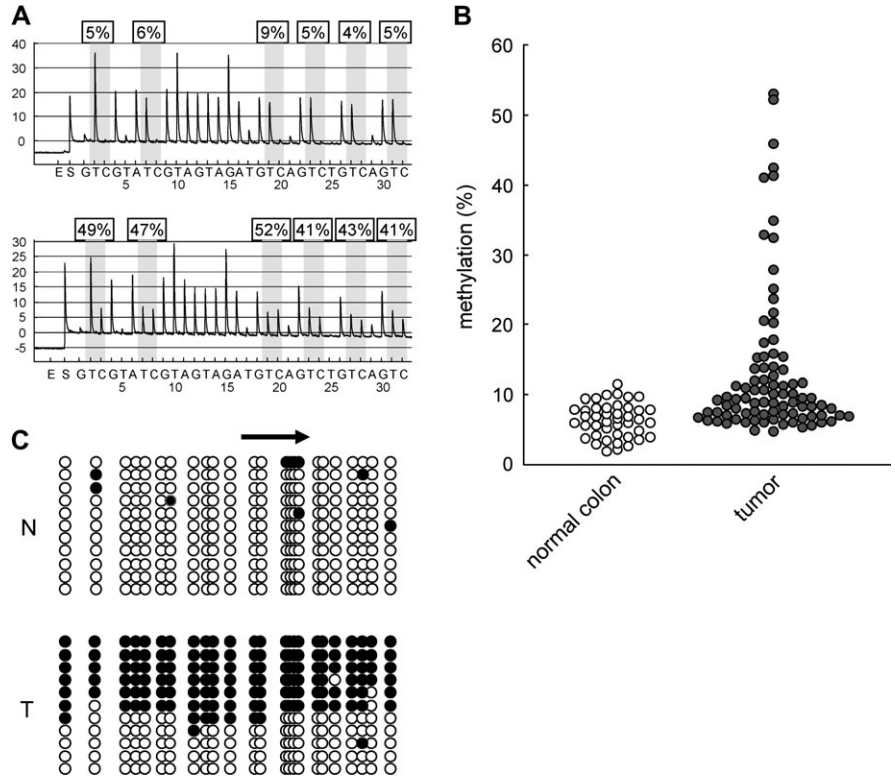

Fig. 4. Analysis of *IGFBP7* methylation in primary colorectal tumors. (**A**) Representative results of pyrosequencing of *IGFBP7*. (**B**) Diagram summarizing the levels of *IGFBP7* methylation detected using pyrosequencing. (**C**) Bisulfite sequencing of *IGFBP7* in primary CRC: Open and filled circles represent unmethylated and methylated CpG sites, respectively: N, normal colon; T, CRC.

p53RE within intron 1 of *IGFBP7* (Figure 3A). p53REs typically consist of two copies of a 10 bp motif (RRRCWWGYYY) separated by 0–12 bp. The putative p53RE for *IGFBP7* (RE-*IGFBP7*) contains a mismatch at a non-critical position within the 20 bp consensus p53-binding sequence (Figure 3A). To determine whether, in fact, p53 directly binds to RE-*IGFBP7*, we carried out ChIP assays using DLD1 cells infected with Ad-p53. After immunoprecipitating DNA–protein complexes from the cross-linked extracts of Ad-p53-infected and control cells using an anti-p53 antibody, we used PCR amplification to measure the abundance of candidate p53REs within the immunoprecipitated complexes. Subsequent ChIP assays confirmed that p53 did indeed bind to DNA fragments containing RE-*IGFBP7* (Figure 3B). To then determine whether p53 can transactivate gene expression via RE-*IGFBP7*, we carried out promoter reporter assays using a luciferase vector containing the wild-type RE-*IGFBP7* sequence upstream of the basal SV40 promoter (pGL3-RE-*IGFBP7*-wt) and a control reporter containing an unresponsive mutated RE-*IGFBP7* sequence (pGL3-RE-*IGFBP7*-mut). H1299 cells, which are null for p53 (29), were transiently cotransfected with one of the reporter plasmids along with a p53 expression vector or an empty vector. In contrast to pGL3-RE-*IGFBP7*-mut, luciferase activity from pGL3-RE-*IGFBP7*-wt was significantly upregulated when cotransfected with a p53 (Figure 3C).

To investigate the effect of p53 on endogenous induction of *IGFBP7*, we assessed expression of *IGFBP7* mRNA in cell lines infected with Ad-p53. Real-time PCR showed that exogenous p53 induced expression of *IGFBP7* mRNA in both H1299 (p53 null, ref. 29) and DLD1 cells (p53 mutant, ref. 30) (Figure 3D). To then assess the role of endogenous p53 in the expression of *IGFBP7*, we treated HCT116 cells with ADR, an agent known to damage DNA and induce endogenous p53 expression, with or without DAC. In a previous study, we showed that ADR, but not DAC, activated p53 and that typical p53 target genes were significantly induced by ADR alone (14,31). However, because *IGFBP7* is methylated and silenced in HCT116 cells, ADR alone could not induce expression of *IGFBP7* mRNA. In contrast, a low dose of DAC (0.1 μM) did induce its expression, and we observed further upregulation *IGFBP7* transcription upon addition of ADR (Figure 3E). When we treated $p53^{-/-}$ HCT116 cells with the same low dose of DAC, the induction was quite weak, and no synergistic upregulation was seen upon addition of ADR (Figure 3E).

To determine the extent to which responsiveness to p53 is affected by methylation in the region around the p53REs, we assessed the methylation status of CpG sites in the vicinity of the p53REs. We found that the region around p53REs was methylated regardless of gene expression. Moreover, this region was also methylated in normal tissues, suggesting that methylation of p53REs does not affect the binding of p53 (supplementary Figure 2 is available at *Carcinogenesis* Online). Taken together, these observations support the idea that *IGFBP7* is a direct target of p53, and its induction can be blocked by DNA hypermethylation.

Growth suppressive effect of IGFBP7

To test whether *IGFBP7* suppresses CRC cell growth, we cloned the full-length *IGFBP7* cDNA into pcDNA3.1 vector, after which we transfected HCT116 cells with the resultant pcDNA3.1His-IGFBP7 vector and verified secretion of the expressed IGFBP7 protein into the conditioned medium (supplementary Figure 1A is available at *Carcinogenesis* Online). We then tested the transfectants in colony formation assays and found that overexpression of IGFBP7 markedly suppressed colony formation (supplementary Figure 1B and C is available at *Carcinogenesis* Online).

Correlation between IGFBP7 methylation and other epigenetic/genetic alterations in CRC and adenoma

We next analyzed the methylation of the *IGFBP7* CpG island in a panel of tumor specimens from CRC patients. Because MSP

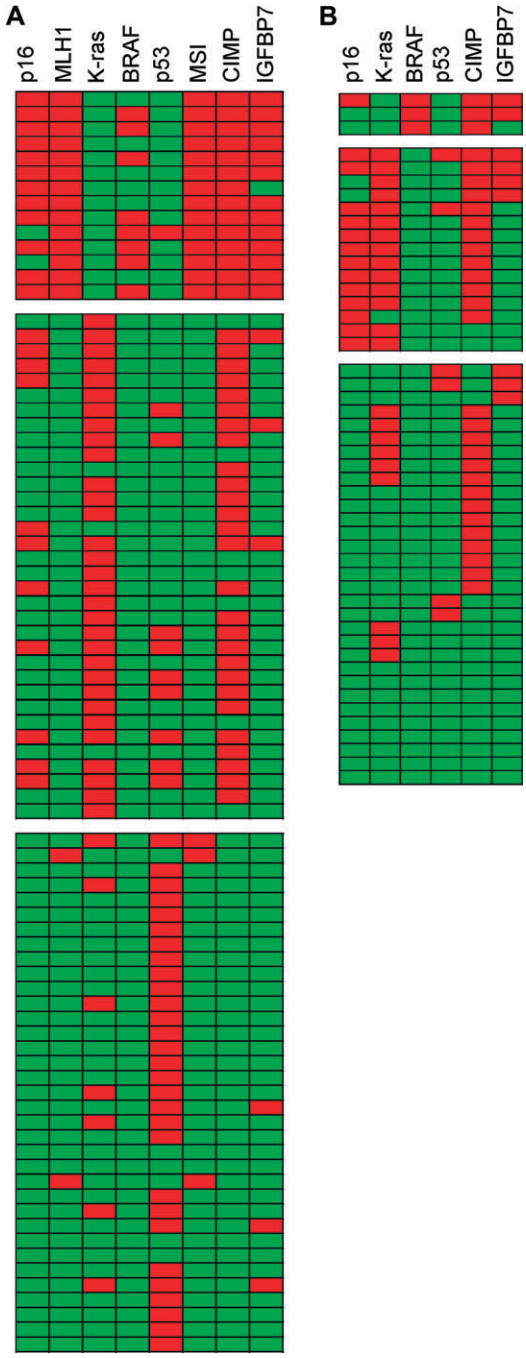

Fig. 5. Epigenetic and genetic alterations in CRCs (**A**) and colorectal adenomas (**B**). K-means clustering analysis based on epigenetic and genetic alterations. Each column represents the separate gene locus shown on the top. Each row is a primary CRC or adenoma: red rectangles, methylated/mutated tumors; green rectangles, unmethylated/wild-type tumors. Fifteen percent methylation was used as the cutoff criterion for methylation of *IGFBP7*.

revealed a low level of *IGFBP7* methylation in normal colonic mucosa, we carried out bisulfite pyrosequencing to quantitatively analyze *IGFBP7* methylation (Figure 4A). As summarized in Figure 4B, levels of *IGFBP7* methylation were significantly higher in primary tumors than in normal colonic tissue ($P < 0.001$). We confirmed these results with bisulfite sequencing in selected specimens. In normal colonic tissue, the vast majority of the CpG island was unmethylated (Figure 4C). On the other hand, tumor tissue in which elevated methylation was detected showed a mixture of entirely and partially

Table I. Correlation between methylation of IGFBP7 and other epigenetic and genetic alterations

		IGFBP7 methylation		
		Mean values	SD	*P*
Age		$R = 0.117$		0.292
Sex	F (25)	14.3	13.2	0.563
	M (58)	12.8	9.4	
p16	Unmethylated (60)	10.2	6.1	0.002
	Methylated (23)	21.4	15.1	
hMLH1	Unmethylated (67)	9.7	4.5	<0.001
	Methylated (16)	28.4	15.0	
K-ras	Wild-type (45)	16.7	13.1	0.001
	Mutated (38)	9.2	3.7	
BRAF	Wild-type (75)	11.0	7.3	0.001
	Mutated (8)	35.2	12.5	
p53	Wild-type (44)	16.4	13.1	0.003
	Mutated (39)	9.8	5.0	
MSI	Stable (66)	9.7	4.5	<0.001
	Unstable (17)	27.2	15.3	
CIMP	Absent (42)	9.6	4.8	0.002
	Present (41)	17.0	13.4	

methylated alleles and unmethylated alleles, probably reflecting contamination of the sample by normal cells (Figure 5C).

Finally, we examined the correlation between *IGFBP7* methylation and other genetic and epigenetic alterations in CRCs (Figure 5A, Table I). We found that there are significant correlations between levels of *IGFBP7* methylation and methylation of *p16* ($P < 0.001$) and *hMLH1* ($P < 0.001$), mutation of *BRAF* ($P < 0.001$), CIMP ($P = 0.002$) and microsatellite instability ($P < 0.001$). Levels of *IGFBP7* methylation were inversely correlated with mutation of *K-ras* ($P = 0.001$) and *p53* ($P = 0.014$). Of 49 colorectal adenomas, nine (18%) showed *IGFBP7* methylation and three (6%) showed *BRAF* mutation, while none showed *hMLH1* methylation or microsatellite instability, indicating that inactivation of *IGFBP7* is an early event in colorectal tumorigenesis (Figure 5B).

Discussion

A subset of CRCs show methylation of multiple CpG islands, indicating that these tumors have CIMP (5). CRCs with CIMP are closely associated with microsatellite instability through methylation of *hMLH1* (5) and frequently show *BRAF* mutations (8), which indicates that these tumors arise via distinct pathways that differ from classical multistep tumorigenesis (6). In the present study, we found that methylation of *IGFBP7* is strongly associated with *BRAF* mutation and the presence of CIMP. Moreover, the earlier finding that *BRAF* mutations are common in hyperplastic polyps and serrated adenomas suggests CRCs with CIMP/*IGFBP7* methylation arise via the serrated pathway (32). It is also known that Ras-mediated epigenetic silencing of effectors, including DNMT1, plays a key role in cellular transformation (33) and that DNMT1 is a downstream target of the Ras-signaling pathway (34). This suggests that *BRAF* activation may be involved in the CIMP phenotype through activation of the DNA methylation machinery. Because the colorectal adenomas examined in this study were not serrated adenomas, further study will be necessary to determine the incidence of *IGFBP7* methylation among serrated adenomas.

It remains unclear why CIMP is associated with *BRAF* mutation. Mutations leading to *BRAF* activation are found in several types of human tumors. Substituting a glutamic acid for a valine at position 600 (BRAFV600E) substantially increases BRAF's protein kinase activity, leading to constitutive extracellular signal-regulated kinase signaling (35,36). However, activation of BRAFV600E does not fully transform primary human cells, indicating that additional cooperative events are required for tumorigenesis (37). Indeed, expression of BRAFV600E induces senescence in cultured primary human

melanocytes (37). And although BRAF mutations are frequently seen in colorectal hyperplastic polyps, these tumors undergo senescence (38). It has therefore been speculated that genes involved in the induction of senescence by BRAF are altered during the progression of tumors. In addition, IGFBP7 was recently shown to play an important role in Ras-mediated senescence (19). Our results thus suggest that CRCs with CIMP may escape senescence by both activating oncogenic signaling (e.g. *BRAF* mutations) and inactivating regulators of senescence (e.g. *IGFBP7* methylation).

The regulatory mechanisms controlling *IGFBP7* expression are not fully understood. p53 is a transcription factor that activates expression of genes involved in cell cycle checkpoints, apoptosis and DNA repair (39). Although CRCs with CIMP show only a low frequency of p53 mutations, the function of p53 may nonetheless be impaired in these tumors due to epigenetic inactivation of target genes, including *IGFBP* family members such as *IGFBP7* and *IGFBP3* (40). Consistent with that idea, several targets of p53 are known to be silenced by DNA methylation (20,41,42). In the present study, we found that *IGFBP7* is not expressed in HCT116 cells but that expression could be restored by treating the cells with DAC. Moreover, Ad-p53 acts synergistically with DAC to further upregulate *IGFBP7* expression. These findings suggest that combining a DNA methyltransferase inhibitor with drugs that induce p53-dependent growth inhibition may be a useful approach to treating CRC. In fact, Lin *et al.* (43) recently reported that reactivation of IGFBP7 using DAC inhibits CRC cell growth.

Weak methylation of *IGFBP7* was even detected in DKO2 cells. Although DKO2 cells lack both DNMT1 and DNMT3B, this cell line does express a different DNA methyltransferase, DNMT3A, which may maintain the observed methylation. Alternatively, residual activity of truncated DNMT1 may be sufficient to maintain the low level of *IGFBP7* methylation seen in DKO2 cells (44). In addition, expression of *IGFBP7* was not fully restored by DAC treatment in HT29 and RKO cells (Figure 1B), which suggests that other cofactors involved in induction of *IGFBP7* also may be impaired in these cell lines.

The molecular mechanism by which IGFBP7 contributes to tumor suppression is not fully understood, though IGFBP7 has been shown to suppress cell growth and induce apoptosis (45,46). In lung and prostate cancers, for example, IGFBP7 induces apoptosis by upregulating expression of Caspase-3 (47,48). On the other hand, knocking down IGFBP7 had no effect on cell growth *in vitro*, though IGFBP7 did suppress anchorage-independent and *in vivo* cell growth (49), suggesting that the effects of IGFBP7 on cell growth vary depending upon the cell type. IGFBP7 is a cell adhesion factor that promotes cell adhesion by binding to cell surface heparin sulfate proteoglycans (50,51). Because CRCs showing expression of IGFBP7 do not grow *in vivo*, Sato *et al.* (49) proposed that although IGFBP7 is involved in cell adhesion, it suppresses anchorage-dependent cell growth *in vivo*. Further study will be necessary to clarify the mechanism by which IGFBP7 modulates growth signaling pathways to suppress the growth of cancer cells.

In summary, we found that *IGFBP7* is a direct target of p53, indicating that IGFBP7 is a mediator of p53-dependent growth suppression. DAC and Ad-p53 acted synergistically to induce *IGFBP7* expression in CRC cells where it was otherwise silenced by methylation. We also found that *IGFBP7* methylation is associated with the *BRAF* mutations, the absence of p53 mutations and the presence of CIMP in CRCs. Thus, epigenetic inactivation of *IGFBP7* appears to be a potentially useful molecular target for the diagnosis and treatment of CRCs with CIMP.

Supplementary material

Supplementary Figures 1 and 2 and Table 1 can be found at http://carcin.oxfordjournals.org/

Funding

Grants-in-Aid for Scientific Research on Priority Areas from the Ministry of Education, Culture, Sports, Science and Technology (K.I., T.T. and M.T.); Grants-in-Aid for Scientific Research (S) from Japan Society for Promotion of Science (K.I.); Grant-in-Aid for the Third-term Comprehensive 10 year Strategy for Cancer Control; Grant-in-Aid for Cancer Research from the Ministry of Health, Labor, and Welfare, Japan (M.T.).

Acknowledgements

The authors thank Dr William F.Goldman for editing the manuscript.

Conflict of Interest Statement: None declared.

References

1. Kinzler,K.W. *et al*. (1996) Lessons from hereditary colorectal cancer. *Cell*, **87**, 159–170.
2. Jones,P.A. *et al*. (2007) The epigenomics of cancer. *Cell*, **128**, 683–692.
3. Kanai,Y. *et al*. (2007) Alterations of DNA methylation associated with abnormalities of DNA methyltransferases in human cancers during transition from a precancerous to a malignant state. *Carcinogenesis*, **28**, 2434–2442.
4. Ushijima,T. *et al*. (2005) Aberrant methylations in cancer cells: where do they come from? *Cancer Sci.*, **96**, 206–211.
5. Toyota,M. *et al*. (1999) CpG island methylator phenotype in colorectal cancer. *Proc. Natl Acad. Sci. USA*, **96**, 8681–8686.
6. Shen,L. *et al*. (2007) Integrated genetic and epigenetic analysis identifies three different subclasses of colon cancer. *Proc. Natl Acad. Sci. USA*, **104**, 18654–18659.
7. Toyota,M. *et al*. (2000) Distinct genetic profiles in colorectal tumors with or without the CpG island methylator phenotype. *Proc. Natl Acad. Sci. USA*, **97**, 710–715.
8. Weisenberger,D.J. *et al*. (2006) CpG island methylator phenotype underlies sporadic microsatellite instability and is tightly associated with BRAF mutation in colorectal cancer. *Nat. Genet.*, **38**, 787–793.
9. Serrano,M. *et al*. (1997) Oncogenic ras provokes premature cell senescence associated with accumulation of p53 and p16INK4a. *Cell*, **88**, 593–602.
10. Zhu,J. *et al*. (1998) Senescence of human fibroblasts induced by oncogenic Raf. *Genes Dev.*, **12**, 2997–3007.
11. Kortlever,R.M. *et al*. (2006) Plasminogen activator inhibitor-1 is a critical downstream target of p53 in the induction of replicative senescence. *Nat. Cell Biol.*, **8**, 877–884.
12. Qian,Y. *et al*. (2008) DEC1, a basic helix-loop-helix transcription factor and a novel target gene of the p53 family, mediates p53-dependent premature senescence. *J. Biol. Chem.*, **283**, 2896–2905.
13. el-Deiry,W.S. (1998) Regulation of p53 downstream genes. *Semin. Cancer Biol.*, **8**, 345–357.
14. Maruyama,R. *et al*. (2006) Comparative genome analysis identifies the vitamin D receptor gene as a direct target of p53-mediated transcriptional activation. *Cancer Res.*, **66**, 4574–4583.
15. Burger,A.M. *et al*. (1998) Down-regulation of T1A12/mac25, a novel insulin-like growth factor binding protein related gene, is associated with disease progression in breast carcinomas. *Oncogene*, **16**, 2459–2467.
16. Landberg,G. *et al*. (2001) Downregulation of the potential suppressor gene IGFBP-rP1 in human breast cancer is associated with inactivation of the retinoblastoma protein, cyclin E overexpression and increased proliferation in estrogen receptor negative tumors. *Oncogene*, **20**, 3497–3505.
17. Lin,J. *et al*. (2007) Methylation patterns of IGFBP7 in colon cancer cell lines are associated with levels of gene expression. *J. Pathol.*, **212**, 83–90.
18. Yamashita,S. *et al*. (2006) Chemical genomic screening for methylation-silenced genes in gastric cancer cell lines using 5-aza-2′-deoxycytidine treatment and oligonucleotide microarray. *Cancer Sci.*, **97**, 64–71.
19. Wajapeyee,N. *et al*. (2008) Oncogenic BRAF induces senescence and apoptosis through pathways mediated by the secreted protein IGFBP7. *Cell*, **132**, 363–374.
20. Toyota,M. *et al*. (2008) Epigenetic silencing of microRNA-34b/c and B-cell translocation gene 4 is associated with CpG island methylation in colorectal cancer. *Cancer Res.*, **68**, 4123–4132.
21. Rhee,I. *et al*. (2002) DNMT1 and DNMT3b cooperate to silence genes in human cancer cells. *Nature*, **416**, 552–556.
22. Bunz,F. *et al*. (1998) Requirement for p53 and p21 to sustain G2 arrest after DNA damage. *Science*, **282**, 1497–1501.
23. Herman,J.G. *et al*. (1996) Methylation-specific PCR: a novel PCR assay for methylation status of CpG islands. *Proc. Natl Acad. Sci. USA*, **93**, 9821–9826.

24. Sasaki,Y. *et al*. (2003) Identification of the interleukin 4 receptor alpha gene as a direct target for p73. *Cancer Res.*, **63**, 8145–8152.
25. Nojima,M. *et al*. (2007) Frequent epigenetic inactivation of SFRP genes and constitutive activation of Wnt signaling in gastric cancer. *Oncogene*, **26**, 4699–4713.
26. Akino,K. *et al*. (2005) The Ras effector RASSF2 is a novel tumor-suppressor gene in human colorectal cancer. *Gastroenterology*, **129**, 156–169.
27. Eisen,M.B. *et al*. (1998) Cluster analysis and display of genome-wide expression patterns. *Proc. Natl Acad. Sci. USA*, **95**, 14863–14868.
28. Barski,A. *et al*. (2007) High-resolution profiling of histone methylations in the human genome. *Cell*, **129**, 823–837.
29. Chen,J.Y. *et al*. (1993) Heterogeneity of transcriptional activity of mutant p53 proteins and p53 DNA target sequences. *Oncogene*, **8**, 2159–2166.
30. Yu,J. *et al*. (1999) Identification and classification of p53-regulated genes. *Proc. Natl Acad. Sci. USA*, **96**, 14517–14522.
31. Adachi,K. *et al*. (2004) Identification of SCN3B as a novel p53-inducible proapoptotic gene. *Oncogene*, **23**, 7791–7798.
32. Minoo,P. *et al*. (2007) Prognostic significance of mammalian sterile20-like kinase 1 in colorectal cancer. *Mod. Pathol.*, **20**, 331–338.
33. Gazin,C. *et al*. (2007) An elaborate pathway required for Ras-mediated epigenetic silencing. *Nature*, **449**, 1073–1077.
34. Bakin,A.V. *et al*. (1999) Role of DNA 5-methylcytosine transferase in cell transformation by fos. *Science*, **283**, 387–390.
35. Davies,H. *et al*. (2002) Mutations of the BRAF gene in human cancer. *Nature*, **417**, 949–954.
36. Rajagopalan,H. *et al*. (2002) Tumorigenesis: RAF/RAS oncogenes and mismatch-repair status. *Nature*, **418**, 934.
37. Michaloglou,C. *et al*. (2005) BRAFE600-associated senescence-like cell cycle arrest of human naevi. *Nature*, **436**, 720–724.
38. Minoo,P. *et al*. (2006) Senescence and serration: a new twist to an old tale. *J. Pathol.*, **210**, 137–140.
39. Riley,T. *et al*. (2008) Transcriptional control of human p53-regulated genes. *Nat. Rev. Mol. Cell Biol.*, **9**, 402–412.
40. Buckbinder,L. *et al*. (1995) Induction of the growth inhibitor IGF-binding protein 3 by p53. *Nature*, **377**, 646–649.
41. Suzuki,H. *et al*. (2000) Inactivation of the 14-3-3 sigma gene is associated with 5′ CpG island hypermethylation in human cancers. *Cancer Res.*, **60**, 4353–4357.
42. Wales,M.M. *et al*. (1995) p53 activates expression of HIC-1, a new candidate tumour suppressor gene on 17p13.3. *Nat. Med.*, **1**, 570–577.
43. Lin,J. *et al*. (2008) Reactivation of IGFBP7 by DNA demethylation inhibits human colon cancer cell growth *in vitro*. *Cancer Biol. Ther.*, **7**, 1896–1900.
44. Egger,G. *et al*. (2006) Identification of DNMT1 (DNA methyltransferase 1) hypomorphs in somatic knockouts suggests an essential role for DNMT1 in cell survival. *Proc. Natl Acad. Sci. USA*, **103**, 14080–14085.
45. Sprenger,C.C. *et al*. (2002) Over-expression of insulin-like growth factor binding protein-related protein-1(IGFBP-rP1/mac25) in the M12 prostate cancer cell line alters tumor growth by a delay in G1 and cyclin A associated apoptosis. *Oncogene*, **21**, 140–147.
46. Wilson,H.M. *et al*. (2002) Insulin-like growth factor binding protein-related protein 1 inhibits proliferation of MCF-7 breast cancer cells via a senescence-like mechanism. *Cell Growth Differ.*, **13**, 205–213.
47. Chen,Y. *et al*. (2007) Insulin-like growth factor binding protein-related protein 1 (IGFBP-rP1) has potential tumour-suppressive activity in human lung cancer. *J. Pathol.*, **211**, 431–438.
48. Mutaguchi,K. *et al*. (2003) Restoration of insulin-like growth factor binding protein-related protein 1 has a tumor-suppressive activity through induction of apoptosis in human prostate cancer. *Cancer Res.*, **63**, 7717–7723.
49. Sato,Y. *et al*. (2007) Strong suppression of tumor growth by insulin-like growth factor-binding protein-related protein 1/tumor-derived cell adhesion factor/mac25. *Cancer Sci.*, **98**, 1055–1063.
50. Akaogi,K. *et al*. (1994) Cell adhesion activity of a 30-kDa major secreted protein from human bladder carcinoma cells. *Biochem. Biophys. Res. Commun.*, **198**, 1046–1053.
51. Sato,J. *et al*. (1999) Identification of cell-binding site of angiomodulin (AGM/TAF/Mac25) that interacts with heparan sulfates on cell surface. *J. Cell. Biochem.*, **75**, 187–195.

Received March 7, 2009; revised June 21, 2009; accepted July 17, 2009